ChemBioChem

Research Article
doi.org/10.1002/cbic.202400279

Chemistry Europe
European Chemical Societies Publishing

www.chembiochem.org

The Dynamic Plasticity of *P. aeruginosa* CueR Copper Transcription Factor upon Cofactor and DNA Binding

Ameer Yasin[+],[a] Alysia Mandato[+],[b] Lukas Hofmann,[a] Yasmin Igbaria-Jaber,[a] Yulia Shenberger,[a] Lada Gevorkyan-Airapetov,[a] Sunil Saxena,*[b] and Sharon Ruthstein*[a]

Bacteria use specialized proteins, like transcription factors, to rapidly control metal ion balance. CueR is a Gram-negative bacterial copper regulator. The structure of *E. coli* CueR complexed with Cu(I) and DNA was published, since then many studies have shed light on its function. However, *P. aeruginosa* CueR, which shows high sequence similarity to *E. coli* CueR, has been less studied. Here, we applied room-temperature electron paramagnetic resonance (EPR) measurements to explore changes in dynamics of *P. aeruginosa* CueR in dependency of copper concentrations and interaction with two different DNA promoter regions. We showed that *P. aeruginosa* CueR is less dynamic than the *E. coli* CueR protein and exhibits much higher sensitivity to DNA binding as compared to its *E. coli* CueR homolog. Moreover, a difference in dynamical behavior was observed when *P. aeruginosa* CueR binds to the *copZ2* DNA promoter sequence compared to the *mexPQ-opmE* promoter sequence. Such dynamical differences may affect the expression levels of CopZ2 and MexPQ-OpmE proteins in *P. aeruginosa*. Overall, such comparative measurements of protein-DNA complexes derived from different bacterial systems reveal insights about how structural and dynamical differences between two highly homologous proteins lead to quite different DNA sequence-recognition and mechanistic properties.

Introduction

Pseudomonas aeruginosa, a pathogen opportunistic to humans, poses a significant threat according to various global health authorities. In response, the World Health Organization (WHO) has actively promoted the exploration and design of new antibiotic classes with distinct targets and modes of action. This initiative aims to mitigate the risk of developing cross-resistance to existing antibiotics. The cohabitation of humans and *P. aeruginosa* fosters the expression of its virulence factors and facilitates its continual adaption to antibiotic resistance.[1] This symbiotic relationship may stem from the bacterium's capability to metabolize various substances such as oils, waste, and pesticides, as well as its inherent resilience to heavy metals.[2] One promising avenue involves disrupting copper homeostasis in *P. aeruginosa*, as this mechanism differs from that of the human host. Remarkably, copper retains its biocidal properties over millennia, making it an interesting target for combating *P. aeruginosa* infections.[3]

Copper ions are essential for many cellular processes, but high concentrations of copper can lead to cell-death.[4] Therefore, *P. aeruginosa* has evolved sophisticated mechanisms to maintain copper homeostasis. This copper regulation system is comprised of various proteins, including chaperones, transporters, cytoplasmic and membrane proteins, and transcription factors. The protein CueR is the first responder to elevated copper levels. CueR is a cytosolic transcription factor belonging to the family of mercury resistance operon regulatory protein (MerR) transcription factors.[4a,5] The occurrence of even miniscule quantities of free copper leads to the rapid activation of CueR in both *P. aeruginosa* and *E. coli*,[5–6] which leads to the initiation of remediation mechanisms. Despite the high sequence similarity of 64% and a sequence identity of 47% between CueR protein in the two organisms, there are clear biochemical differences (Figure 1). First, the affinity of Cu(I) to *E. coli* CueR is higher than that of *P. aeruginosa* CueR. The reported dissociation constants are $K_D = 10^{-21}$ M to $3.25 \cdot 10^{-19}$ M[6–7] for *E. coli* versus $K_D = 2.5 \cdot 10^{-16}$ M for *P. aeruginosa* CueR.[5b] Second, activation of *P. aeruginosa* CueR upon complexation of Cu(I) increases transcription levels of at least five proteins: *copZ1/2, mexPQ-opmE (PA3521–3523), copA1 (PA3920)*, and *PA3515–3519*,[8] while the activation of *E. coli* CueR facilitates the expression of only two genes, *copA* and *cueO*. Finally, the calculated isoelectric point (pI) of *P. aeruginosa* CueR is 7.73 compared to 5.72 for *E. coli* CueR.[9]

Nevertheless, the biochemical process for gene expression of proteins that ameliorate the high Cu(I) concentration is the same for both organisms. CueR binds to the promoter and

[a] *A. Yasin,[+] Dr. L. Hofmann, Y. Igbaria-Jaber, Dr. Y. Shenberger, Dr. L. Gevorkyan-Airapetov, Prof. S. Ruthstein*
Department of Chemistry and the Institute of Nanotechnology and Advanced Materials
Bar-Ilan University
Ramat-Gan, Israel, 5290002.
E-mail: Sharon.ruthstein@biu.ac.il

[b] *A. Mandato,[+] Prof. S. Saxena*
Department of Chemistry
University of Pittsburgh
Pittsburgh, PA, 15260
E-mail: sksaxena@pitt.edu

[+] *Equal contribution*

Supporting information for this article is available on the WWW under https://doi.org/10.1002/cbic.202400279

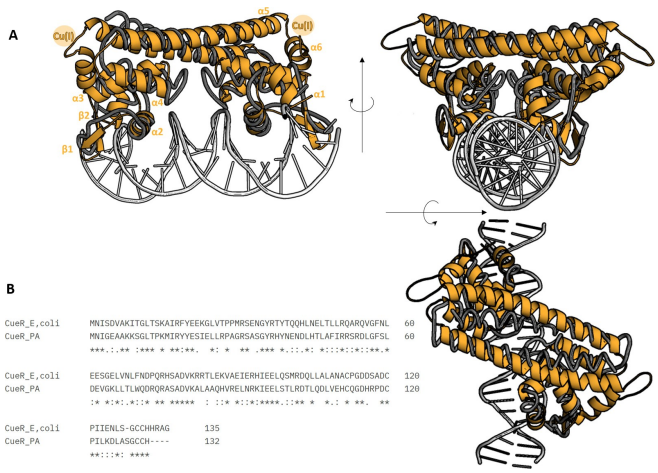

Figure 1. A. *E. coli* CueR structure (PDB 1Q05) in grey and structural model of *P. aeruginosa* CueR (orange) based on 1Q05 structure. **B**. CueR sequence alignment between *E. coli* and *P. aeruginosa* generated by Clustal Omega (EBI) revealing high similarity of 64 %, and 47 % sequence identity, including a significant difference in the C-terminus of *P. aeruginosa* CueR.

bends the DNA so that RNA polymerase can access the gene to start transcription.[10] The complexation of Cu(I) to CueR enables DNA binding and activates transcription.[5a,11] The X-ray structure of *E. coli* CueR has been resolved in the presence of Cu(I).[6,12] The protein is a homodimer, and each monomer consists of six helices and two β-sheets (Figure 1). We recently showed that EPR spectroscopy is an effective tool to study this transcription mechanism in *E. coli*.[11b,13] EPR can follow the conformational and, even more interestingly, site-specific dynamical changes in a Cu(I) concentration dependent manner and DNA binding in solution.[13a–c] With EPR measurements, we were able to systematically examine the *E. coli* CueR protein in different functional states and elucidate essential properties about the mechanism of metal regulation. More specifically, we detected significant structural changes of *E. coli* CueR in solution in comparison to the Cu(I)-CueR-DNA complex.[11b,13a–c] In the Cu(I)-CueR-DNA complex (i.e., the active state) we detected two different conformations of *E. coli* CueR complexed to Cu(I) and DNA. Furthermore, these experiments demonstrated that Cu(I) drives these conformational and dynamical changes, if bound to DNA. Using titration experiments at room temperature (RT) in dependency of Cu(I) and DNA binding, we revealed that *E. coli* CueR holds two different Cu(I) binding sites. When both sites are occupied with Cu(I), the dynamics of helices in the DNA- and copper-binding domains increase, which potentially leads to inactivation of the transcription process.[13a] When only one Cu(I) site is occupied via coordination to C112 and C120 residues, the protein is rigid and tightly bound to the DNA, which allows for activation of transcription.

Herein, we apply RT EPR measurements on *P. aeruginosa* CueR to follow dynamical changes in different regions of the protein in dependency of Cu(I) and DNA binding. We compared the binding of CueR to two different DNA promoter sequences: *mexPQ-opmE* and *copZ2*. MexPQ-OpmE is a member of the family of resistance-nodulation-cell-division (RND)-type multidrug efflux pumps, and its transcription level is controlled by CueR.[8c] Hence, the results shed light on the interplay between heavy metal homeostasis and multidrug resistance.[14] CopZ2 is a copper chaperone that transports copper to different cytoplasmic proteins within the bacteria. We showed that the transcription mechanism of CueR depends not only on the DNA sequence, but also on the species itself. Distinct differences were detected between the mechanism of *E. coli* CueR described previously[13a] versus the mechanism of *P. aeruginosa* CueR. This work highlights the sensitivity of the transcription initiation mechanism to both the protein and DNA sequences.

Results

P. aeruginosa CueR (PA_CueR/PCueR) was expressed and purified as described in the Experimental Section and the SI (Figure S1, SI). Electrophoretic mobility shift assay (EMSA) experiments were employed to explore the binding of PA_CueR with both *mexPQ-opmE (mexPQ)* and *copZ2* DNA (Figure 2). The EMSA gels show two different bands for the protein-DNA complexes, which suggests the presence of a higher oligomerization state of PA_CueR in the DNA-bound state. Similar

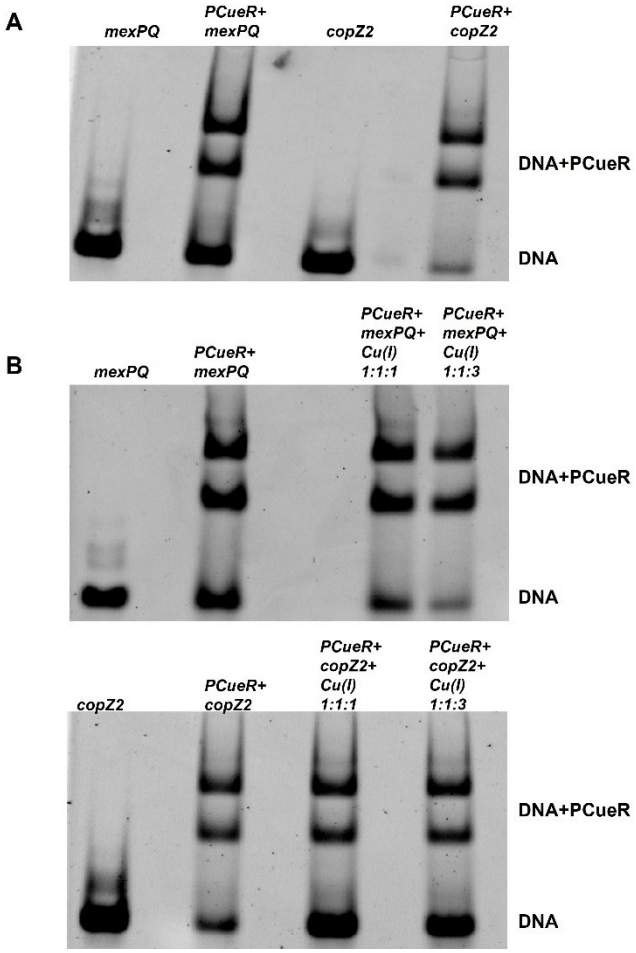

Figure 2. EMSA gel of WT PCueR as a function of **A**. *mexPQ* and *copZ2* binding, **B**. *mexPQ* and *copZ2* and Cu(I) binding.

observations of higher regulator oligomerization were recently reported for the zinc uptake regulator (Zur) of *Streptomyces coelicolor*.[15] In addition, SEC-HPLC data (Figure S2, SI) showed that PA_CueR can exist both as a dimer as well as a tetramer in solution and in the protein-DNA complexes. Interestingly, PA_CueR binds *copz2* with higher affinity than *mexPQ*. If complexed with Cu(I), however, the affinity to *copZ2* decreases while the affinity to *mexPQ* increases. Interestingly, such higher oligomerization was not observed to the same extent for the *E. coli* CueR homolog.[11b,13a,c,16] These results suggest that discrepancies between the two homologs are beyond the sequence identity and are reflected by the different activities of these metalloregulators.

In order to follow differences in dynamics of PA_CueR in dependency of Cu(I) and DNA, RT continuous wave (CW) EPR experiments were applied. RT CW-EPR measurements coupled with nitroxide spin labeling have been employed for decades to observe site-specific dynamics of biomolecules.[17] In this methodology, a macromolecule is site-specifically labeled with a small free radical and then the mobility of the spin label is evaluated from the EPR line shape. For surface-exposed helical sites and loops, changes in EPR line shapes are assigned to differences in site-specific backbone dynamics, which then can be inferred to a biological function.[17c,d,18] The most common spin label is S-(2,2,5,5-tetramethyl-2,5-dihydro-1H-pyrrol-3-methyl) methanethiosulfonate (MTSSL) which is covalently bound to cysteine residues and has only a minor impact on the structure of the protein (Figure 3).[19]

PA_CueR has four cysteine residues: C112 and C120 which compose the Cu(I)-binding site, and C130 and C131 at the C-terminal domain. For our experiments we maintained C112 and C120, but mutated C130 and C131 to alanine residues to avoid spin labeling at these sites. Three Cys mutants were prepared and spin labeled: PA_CueR_G11C, PA_CueR_A33C, and PA_CueR_G57C (Figure 3).To prevent spin labeling at the copper binding site, spin labeling was carried out in the presence of copper as described previously[13b,c] and in the Experimental Section. Subsequently, bound copper was removed by several dialysis steps, and KCN was used to show that no Cu(I) was present. The first two mutants (i.e., G11C and A33C) are located within the DNA-binding domain, while G57C is located on a loop between the DNA-binding domain and the copper-binding domain. After successful spin labeling with MTSSL, the spin labeling sites were termed R1. Data from HPLC and CD demonstrated that labeling and mutations do not affect the protein's oligomerization and secondary structure elements (see Figures S2 and S3).

Figure 4A illustrates the CW-EPR spectra for the three different R1 mutants in the apo-state. Visual analysis of the apo-states shows differences in site-specific dynamics at different locations. These differences are mostly dominate at the central field absorption peak (ca. 3520 G). For instance, PA_CueR _ G57R1 is much broader than the two other mutants, indicative of restricted motion at this loop region. The A33R1 site has much narrower lines than G57R1, which indicates faster dynamics near the DNA-binding domain.

To improve our understanding of the site-specific dynamical differences, the line shapes were analyzed using the chili function in EasySpin.[20] Most of the spectra could be only simulated using a two-component fit due to the presence of two features that contribute to the overall spectra. For example, in Figure 4A, a broad immobile component (marked as "im") is visible at ca. 3490 G, and a narrow mobile component (marked as "m") is present at ca. 3500 G. The observation of multiple components in a CW-EPR spectrum is common for proteins with R1 spin labels.[13d,21] The simulations were performed by varying the rotational correlation times of the mobile component and the population weights of the immobile and mobile

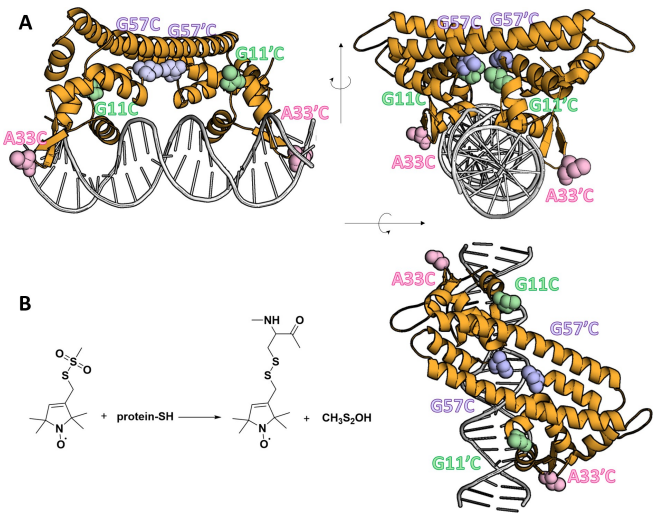

Figure 3. A. Spin labeling of a cysteine residue with methanethiosulfonate (MTSSL). **B**. Site directed spin labeling sites in PCueR.

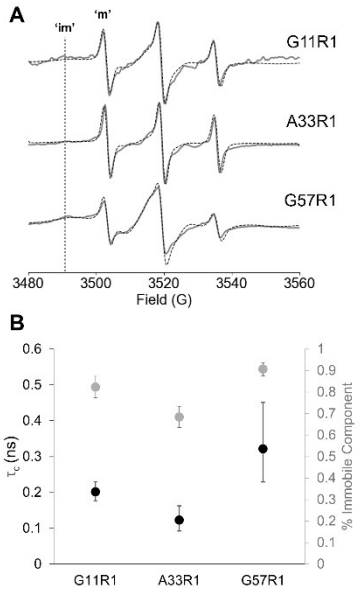

Figure 4. A. RT CW-EPR spectra (solid lines) of three different spin labeled PA_CueR mutants in the apo-state and corresponding simulated data (dotted lines). **B**. The correlation time (black circles) of the mobile component and the contribution of the immobile component (grey circles) based on EasySpin simulations of each PA_CueR mutant. The error bars were obtained directly from the EasySpin.

components. Other parameters, such as line broadening, were kept constant for the simulations. Figure 4B shows the rotational correlation time (τ_c) of the mobile component and the fraction of the immobile component for each site. The simulation parameters are reported in Tables S1–S3, SI, and all the simulated spectra are provided in Figures S4–S12, SI.

Consistent with the CW-EPR line shapes, the A33R1 site has the shortest correlation time for the mobile component and the lowest percentage of the immobile component, indicating that this site has the fastest backbone dynamics. In contrary, the G57R1 site is described by a long correlation time of the mobile component and a high percentage of immobile component, making it the most dynamically restricted site of the three.

The behavior of PA_CueR _G57R1 is different than the *E. coli* CueR_G57R1 site that was previously reported.[13a] In *E. coli*, this site was characterized by high dynamics,[13a] where in *P. aeruginosa*, the motion at this site is restricted, which suggests differences in dynamics between the two homologs in this region. Since the A33R1 site is at the DNA-binding domain on a link between the two β strands, it is reasonable that it is the most dynamic site on the protein. A high degree of dynamics allows the protein to rapidly "search" for the DNA-binding site to bind. However, the dynamics of the PA_CueR _G11R1 site which is also in the DNA-binding domain located between α1 and α2 helices, but maybe not in direct contact with the DNA, is comparably restricted. Comparing the dynamics of spin labelled sites in the DNA-binding domain of *E. coli* CueR with PA_CueR suggests that the contribution of the slow component is much higher in PA_CueR (>0.65, Figure 4B), while in *E. coli* CueR it is smaller than 0.5 for different sites in the protein.[13a] This indicates that PA_CueR protein is less dynamic than *E. coli* CueR.

Backbone dynamics in the protein-DNA complexes: At low to stoichiometric protein:DNA ratios, this metalloregulator exists in the repressed state, wherein the DNA is believed to be straight.[11b,12] We next probed site-specific dynamics in this repressed state. The CW-EPR line shapes in the presence and absence of the *copZ2* and *mexPQ* DNA sequences are shown in Figures 5A–C. Qualitatively there is substantial narrowing of the lineshape of the G57R1 site in the complexed state. The changes in line shape for the other two complexes are more modest. Most of the data was again simulated using two components, while the G57R1 mutant bound to *copZ2* DNA was best simulated with one component. The simulation parameters are given in Tables S1–S3, SI, and all the simulated spectra are provided in Figures S4–S12, SI. We were able to achieve good fits only by varying the correlation times of the mobile component and the component weights. The changes in the rotational correlation times of the mobile component and the immobile component weight are provided in Figures 5D–F for each mutant.

Visually, the data suggest only minor changes in line shape if DNA is present for CueR_G11R1 which led to some minor reduction in the correlation time (Figure 5D). In contrast, for G57R1, a large increase in dynamics was detected in combination with DNA, especially in the presence of *copZ2*. Such differences are clearly manifested by a reduction of the line width in the experimental data. For A33R1, a marginal increase in dynamics was detected with *mexPQ*, while a decrease in dynamics was observed with *copZ2* DNA. Interestingly, for all

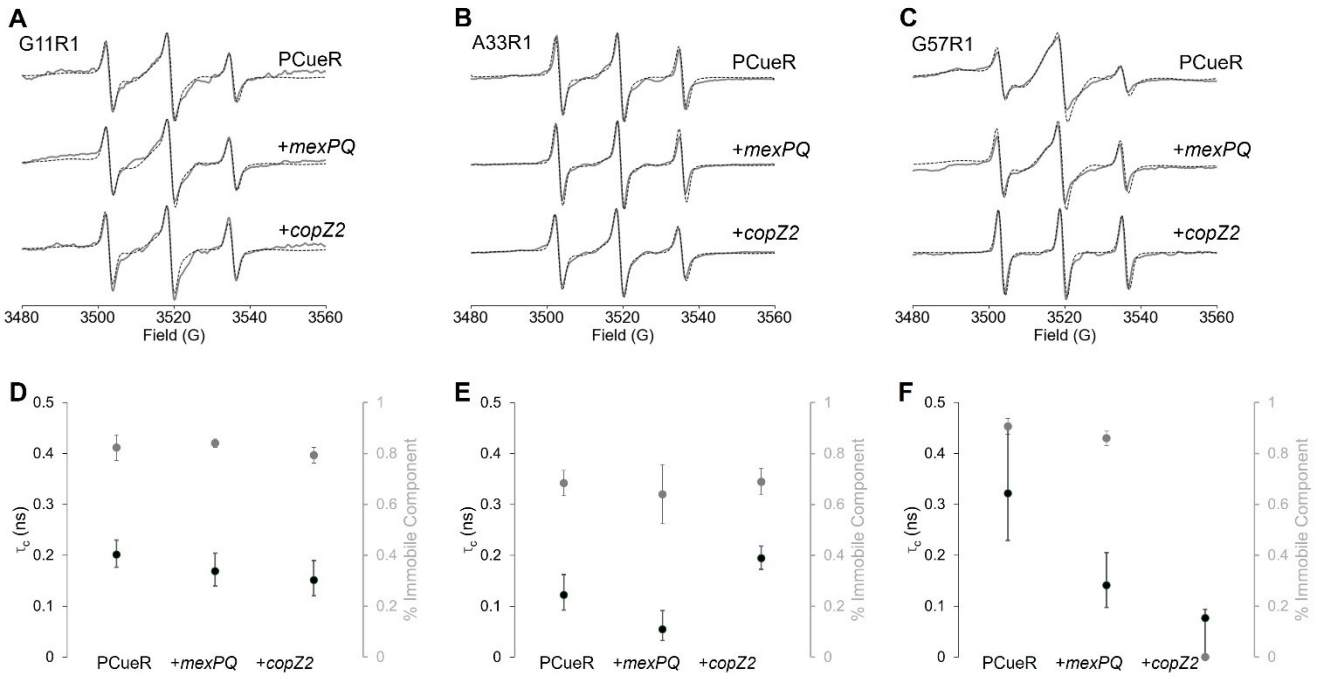

Figure 5. RT CW-EPR spectra in the absence and presence of *mexPQ* and *copZ2* DNA (experimental – solid lines, simulations – dotted lines) for **A**. PCueR_G11R1, **B**. PCueR_A33R1, and **C**. PCueR_G57R1.The change in the correlation time of the mobile component (black circles) and the weight of as the immobile component (grey circles) in dependency of DNA binding for **D**. PCueR_G11R1, **E**. PCueR_A33R1, and **F**. PCueR_G57R1. The error bars were obtained directly from the EasySpin.

sites, the change in dynamics is more significant in the presence of *copZ2* DNA than *mexPQ* DNA. This is interesting, especially given that the EMSA data (Figure 2) suggests that PA_CueR has a higher affinity to *copZ2* than to *mexPQ* DNA in the absence of copper ions.[8c] The change of dynamics in combination with DNA is different than the behavior of *E. coli* CueR,[13a] where the addition of DNA did not change site-specific dynamics in different regions of the protein. The results again emphasize the different dynamical behaviors of the two homologs.

Dynamics in the presence of Cu(I): Mechanistically in combination with Cu(I), the DNA in the protein:DNA complex is distorted to promote the coordination to RNA polymerase. Often this state is referred to as the active state of the protein. To explore these dynamical effects in the active state, systematic experiments were performed and CW-EPR spectra were measured as a function of increasing Cu(I) concentrations for all combinations, solely protein, protein-*mexPQ*, and protein-*copZ2* complexes for all three mutants.

Addition of Cu(I) to PA_CueR _G11R1 did not result in significant changes in the line shapes (Figure 6A, Figure S6, SI) with or without DNA, indicating that this site is less sensitive both to DNA coordination as well as to Cu(I) binding.

For the PA_CueR_A33R1 site (Figure 6B, Figure S7, SI), without DNA, there is an extension of the correlation time (decrease in dynamics) at low copper concentrations, and then stabilization up to 1.5 Cu(I):PA_CueR. However, at a ratio of 2 Cu(I):PA_CueR, a sudden substantial increase in dynamics occurs. In combination with *mexPQ* DNA (Figure 6B, Figures S8, SI), no change in dynamics as a function of copper was observed, however in the presence of *copZ2* DNA (Figure 6B, Figures S9, SI), there is a slight increase in dynamics up to a ratio of 0.7 Cu(I):PA_CueR and then stabilization at higher copper concentrations.

For the PA_CueR_G57R1 site, in the absence of DNA (Figure 6C, Figure S10, SI), there is an increase in dynamics at low copper concentrations up to 0.5 Cu(I):PCueR, and then there are some changes in dynamics between 0.5–2.0 Cu(I):PCueR, and then a stabilization at higher copper concentrations. In the presence of *mexPQ* DNA (Figure 6C, Figure S11, SI), there is a slight decrease in correlation time (increase in dynamics) at low copper concentrations <0.7 Cu(I):CueR and then a stabilization. In the presence of *copZ2* DNA (Figure 6C, Figures S12, SI), there is no change in correlation time of the G57R1 site.

The behavior of the PA_CueR _A33R1 and PA_CueR _G57R1 sites in dependency of copper and without DNA may suggest that there are two copper sites and therefore the stabilization in dynamics appeared only at a ratio of about 2 Cu(I):PA_CueR. For *E. coli* CueR, we observed reduced dynamics between 0.5 to 1.5 Cu(I):CueR ratio, and then a sudden increase in dynamics at a ratio of 2:1 Cu(I):CueR.[13a] Therefore, we concluded that this behavior can only be explained by the existence of two distinct Cu(I) sites in the protein monomer: one between helices α5 and α6, and one at the C-termini in each monomer. Moreover, we hypothesized that binding of copper to the C-termini may lead to repression of the transcription mechanism.[13a] For PA_CueR, the changes in dynamics up to a ratio of 2 Cu(I):PA_CueR were more moderate, and therefore a clear statement of whether there are two distinct Cu(I) sites per monomer cannot be established. Moreover, the PA_CueR is characterized by 130

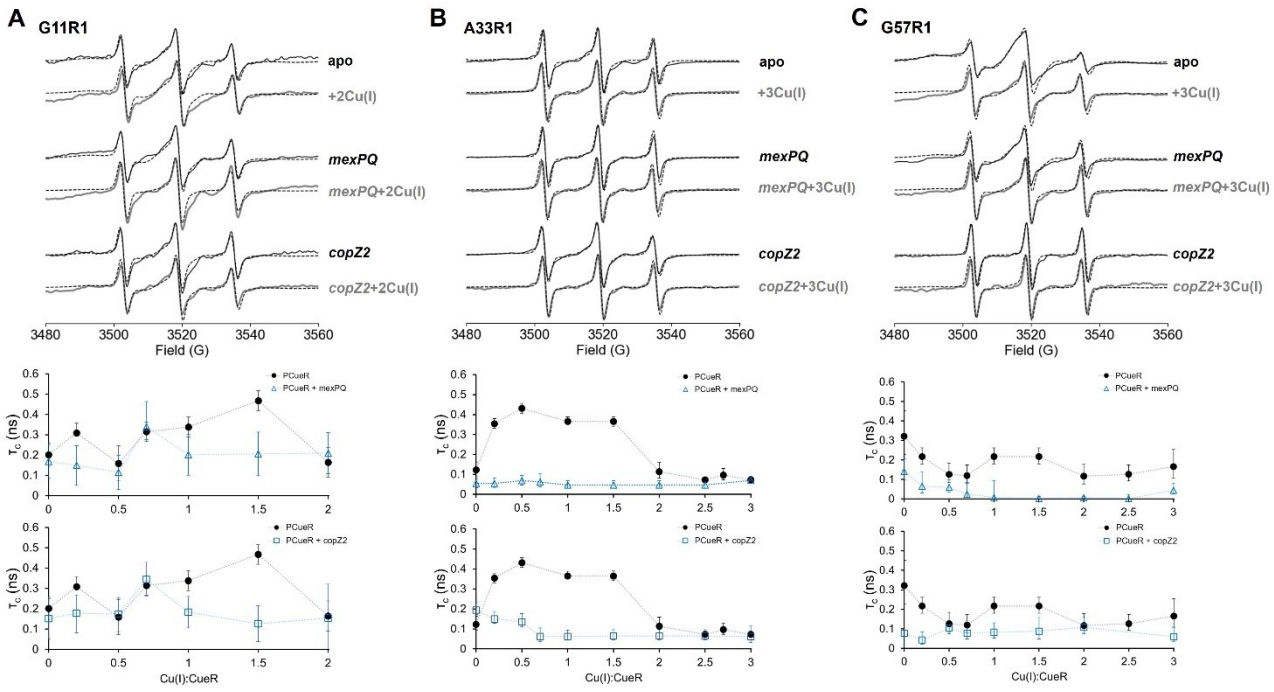

Figure 6. RT CW-EPR experimental (solid line) and simulated spectra (dashed lines) for different PCueR mutants as a function of DNA (*mexPQ/copZ2*) and Cu(I) binding and corresponding correlation time of the mobile component for **A**. PCueR_G11R1, **B**. PCueR_A33R1, and **C**. PCueR_G57R1. The error bars were obtained directly from the EasySpin.

amino acids, where *E. coli* CueR is 135 amino acids. Previously we proposed that the sequence HHRAG at the C-terminus of the *E. coli* protein holds a key role in forming the second Cu(I) site.[13a,22] Interestingly, in PA_CueR this C-terminal motif is missing.

Discussion

The structure of the PA_CueR copper transcription factor from the MerR family has not been resolved yet. Hence, only little is known about the structure-activity relationship of this homolog including its biochemistry. Nonetheless, the structure is known to be similar to *E. coli* CueR because of the high sequence similarity. Herein, we applied RT CW-EPR experiments together with SDSL to measure dynamical differences in the DNA-binding domain of PA_CueR in dependency of copper and two DNA promoters: *copZ2* and *mexPQ-opmE*. Moreover, the acquired data of this study is compared to a previous study performed by us on the *E. coli* CueR.[13a] In general, the CW-EPR spectra suggests that the dynamics of the DNA-binding domain of the PA_CueR protein is slower than the *E. coli* CueR. More interestingly, for *E. coli* CueR, we found that complexing of Cu(I) led to dramatic changes in dynamics of the DNA-binding domain of CueR, which is ca. 30 Angstroms away from the metal-binding domain.[13a] This result led to the inference that in *E. coli* CueR, Cu(I) remediation is initiated by metal binding that leads to tuning of the dynamics of the DNA-binding domain to promote binding to the DNA. On the other hand, only minor alterations in site-specific dynamics were observed at low copper concentrations for PA_CueR.

On the other hand, site-specific dynamical changes were detected in PA_CueR upon binding the DNA, whereas no alterations in dynamics were observed for *E. coli* CueR upon DNA binding. Finally, the dynamics of PA_CueR were affected differently in the presence of *copZ2* compared to *mexPQ*, where larger changes in the dynamics, especially for PA_CueR_G57R1 site, were observed in the presence of *copZ2* than *mexPQ*. Therefore, it seems that PA_CueR is more sensitive to DNA binding as compared to *E. coli* CueR. The observed differences in domain dynamics upon *copZ2* and *mexPQ* binding are aligned with the differences in K_D of *copZ2* and *mexPQ* which are 33 nM and 146 nM, respectively.[8c] Interestingly, the RNA expression levels upon copper stress reveal that *copZ2*-promoter regulated RNA levels increase about 30,000 reads from 5,000 to 35,000 whereas for *mexPQ* a smaller increase from 25 to 5,000 reads is observed.[8a] Taken together, larger differences in dynamics in the G57R1 region upon DNA binding may translate to higher transcription levels of upregulated genes.

These differences in dynamics between *E. coli* CueR and PA_CueR can also be rationalized by the more compact structure of PA_CueR. Figure 7 shows the homology model of PA_CueR. A π–π stacking (Phe49 and Trp70) between helix α3 and helix α4 (Figure 7) is observed, which may provide higher stability in PA_CueR. This interaction is missing in *E. coli* CueR. The presence of this interaction is consistent with the restricted

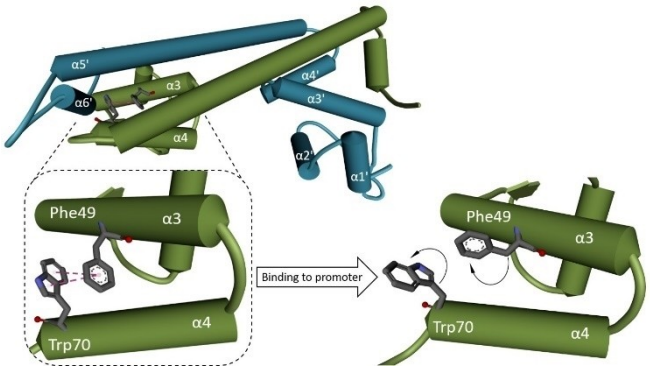

Figure 7. π–π interaction between Phe49 (on α3 helix) and Trp70 (on α4 helix) in PA_CueR. The homology model was generated using the Swiss-Model server based on *E. coli* CueR PDB-ID:1Q05 for the unbound DNA state, and PDB-ID: 4WLS for the DNA-bound state. The homology model indicates that upon DNA binding, the π–π interaction is broken in the repressed state.

motion of G57R1 in PA_CueR and the sensitivity of this region to DNA binding. On the other hand, in *E. coli* the same residue exhibits higher dynamics. Moreover, upon DNA binding, this π–π interaction is weakened, resulting in the observed change in dynamics (Figures S13–S14, SI). Adding copper to the solution when the protein is bound to the DNA did slightly affect the dynamics. This may suggest that once the π–π stacking is disrupted upon binding of the promoter sequence, the dynamics can increase in a gradual manner as a function of copper binding, and therefore the effect on the dynamics of the protein is much lower in the DNA-bound state.

Additionally, the difference in oligomerization states upon promoter binding observed in EMSA may suggest a more refined regulation mechanism for PA_CueR compared to *E. coli* CueR. While for *E. coli* a binding ratio of 1 : 1 DNA to CueR-dimer is predominant, for *P. aeruginosa* a higher oligomer ratio was observed of 1 : 2 DNA to CueR-dimer (Figure 2). These findings are in agreement with other metalloregulators which exhibit more than just one regulatory site per promoter region.[15] Altogether, we hypothesize that PA_CueR is capable of sliding along the DNA and upon binding of the promoter sequence, the reported π–π interaction between helix α3 and α4 breaks and stalls CueR on the promoter sequence, allowing the regulation of transcription levels of RNA as a response to environmental copper.

This comparison study of two close homologs delineated, for the first time, differences in the domain dynamics and oligomerization states of the protein upon DNA binding. Such differences might be essential to the origin of the differences in pathogenicity and resistance of these bacteria. *P. aeruginosa* CueR is a more complex copper sensing system that regulates at least five different proteins, including a multidrug efflux pump which exports disinfecting agents, antiseptics, and various classes of antibiotics such as phenicols, macrolides, tetracyclines, diaminopyrimidine, and carbapenem antibiotics.[14] The higher sensitivity of *P. aeruginosa* CueR to the promoter DNA, as compared to *E. coli* CueR, might potentially lead to the increased resistance of *P. aeruginosa* as compared to *E. coli*.

Moreover, the lack of a second copper binding site and the observation that in the DNA-bound state, the interaction between α3-α4 is weakened which results in changes in dynamics of the protein already at low copper concentrations, may suggest that the activation can occur at significantly lower copper concentrations (below 1 : 1 Cu(I) : PCueR) in *P. aeruginosa* as compared to *E. coli*. Such fine tuning may allow *P. aeruginosa* to share its habitat with humans and to survive even under harsh conditions with the same toolbox as *E. coli* but with more refined equipment.[23]

Conclusions

CW-EPR experiments at RT showed that despite the high sequence similarity between two CueR homologs from different bacterial systems, their dynamical behaviors are different. Such differences likely influence the regulation of gene transcription of proteins contributing to copper homeostasis and multidrug resistance. These detailed insights about the mechanism of action of *P. aeruginosa* CueR and the direct comparison to its closely related homolog in *E. coli* provides clues as to how protein dynamics may contribute to increased resistance and virulence of *P. aeruginosa* CueR compared to *E. coli* on a molecular level. More research is required to fully map the dynamical differences of close homologs to understand phenotypical differences observed in bacteria with a shared toolbox.

Experimental Section

Expression and purification of *P. aeruginosa* CueR (PA_CueR): Wild-type (WT) and PA_CueR mutants were cloned in modified pET28a using PCR. The generated plasmid was confirmed by DNA sequencing. MBP fusion protein and TEV cleavage were added upstream of initiation codon of our protein. After a transformation process of the expression plasmid, *E. coli* BL21 cells were grown in 400 mL of LB media prepared in 1 L flasks (5 times) in a total volume of 2 L. The cells were grown at 37 °C until OD_{600} reached at least 0.8 A, then 200 μL of 1 mM isopropyl-β-D-thiogalactopyranoside (IPTG) were added in each flask. After an overnight growth at 22 °C, the bacterial cells were separated by centrifugation at 8000 rpm for 25 minutes at 4 °C. The pellets were re-suspended in a lysis buffer containing 25 mM Tris-HCl pH 8.5, 250 mM NaCl, 1% Triton-X100 and 20 mM limidazole. The pellets were homogenized and treated with 1 mM dithiothreitol (DTT). A sonication process was carried out with the following parameters: pulse 10s on 10s off; amplitude 35%; time 10 min. An additional centrifugation process at 4 °C for 25 min at 14000 rpm was performed to separate the cell lysate. The supernatant was applied to 5 mL of Ni-NTA beads for a capturing step. Several washes of the resin were performed to purify the PA_CueR followed by an SDS-PAGE gel run and Coomassie staining for confirming protein purification. The cleavage step was performed using TEV protease. The purified wash fraction was incubated with 1 mL of TEV protease (2 mg/mL) overnight in a dialysis bag in 1 L of dialysis solution (25 mM Tris-HCl pH 8.5, 250 mM NaCl, 0.1% Triton-X100) with gentle stirring at 17 °C.

The expression yield of PA_CueR was low (0.01–0.02 mM) compared to the *E. coli* CueR. Especially, the yield of the mutant PA_CueR_G11 C was the lowest, and the stability of the protein at high Cu(I) concentrations was lower, leading to aggregation at high copper concentrations. Table 1 lists all the primers used in this study.

PA_CueR spin labeling: Before spin labeling the protein with S-(2,2,5,5-tetramethyl-2,5-dihydro-1H-pyrrol-3-methyl) methanethiosulfonate (MTSSL, TRC), a DTT treatment was applied to prevent reducing disulfide bonds. PA_CueR was incubated with 1 mM DTT with vigorously shaking (approximately 1000 rpm) at 4 °C for 12 h. To remove free DTT, the reduced protein was transferred to 1 kDa dialysis cassettes for a dialysis process at 4 °C for another 12 h. The PA_CueR mutant protein (250–300 μM) was then incubated overnight with 10-fold excess of MTSSL and 600 μM Cu(I) (Tetrakis (acetonitrile) copper(I) hexafluorophosphate, Sigma-Aldrich) with vigorous shaking at 4 °C. An additional dialysis step was conducted for 72 h at 4 °C to remove free MTSSL.

Cu(I) addition: For EPR measurements, Cu(I) (Tetrakis (acetonitrile) copper(I) hexafluorophosphate, Sigma-Aldrich) was added to the protein solution under anaerobic conditions. No Cu(II) EPR signal was observed at any time.

EPR measurements: Continuous wave EPR (CW-EPR) experiments were performed on X-band E500 Elexsys Bruker spectrometer. The spectra were recorded at RT with microwave power of 20.0 mW, time constant of 60 ms, modulation amplitude of 1.0 G, and a receiver gain of 60 dB. The samples were measured in 0.8 mm capillary quartz tubes (vitrocom).

Electrophoretic Mobility Shift Assay (EMSA) with EtBr stain: Several EMSA experiments were carried out to detect PA_CueR interactions with the DNA sequences, *copZ2* and *mexPQ*, and as a function of Cu(I), at RT for about 30 min in suitable binding buffer (25 mM Tris-HCl pH 8.5, 250 mM NaCl, 5% Glycerol). The DNA sequence of *copZ2* operon is 5′-GGATTGACCTTGACACCATGTCAAGGTCGAAAAT-3′ and *mexPQ* operon DNA sequence is 5′-GGGTTGACCTTGCCAAGGTGTCAAGGTCGATAAC-3′. The gel was performed with TAE buffer (40 mM Tris-HCl, 20 mM acetic acid, 1 mM EDTA) at 4 °C and 80 V for 1 h. The staining of the gel was done using 1 μg/mL ethidium bromide for 15 min and analyzed with a Gel Doc EZ BioRad system.

CW-EPR Simulations: The RT CueR data were simulated using EasySpin and the chili function. The spectra were simulated using two-components (mobile and immobile). The g values were identical for both components: $g_{xx} = 2.0088$, $g_{yy} = 2.0058$, and $g_{zz} = 2.0028$. The mobile component has hyperfine values of $A_{xx} = 16$, $A_{yy} = 16$, and $A_{zz} = 105$ MHz. The immobile component has hyperfine values of $A_{xx} = 16$, $A_{yy} = 16$, and $A_{zz} = 103$ MHz.[22] The β_D parameter for each component was constant at 15°. For each mutant, the exact values of each parameter are provided in Tables S1–S3. The population weights and the rotational correlation times of the mobile component were varied to fit each spectrum. Some of the data sets were fit by keeping the weight of the immobile component constant (i.e., G11R1, A33R1, G57R1 + *copZ2*). All other spectra were fit by varying both the weights and rotational correlation time of the mobile component. The rotational correlation time of the immobile component was kept constants for all simulations.

Circular Dichroism (CD) Characterization: CD experiments were performed using a Chirascan spectrometer (Applied Photophysics, UK) at RT. 1 mm optical path length cell was used. The step size and the bandwidth were 1 nm. Spectra were obtained after background subtraction.

Supporting Information

The authors have cited additional references within the Supporting Information.[24]

Acknowledgements

SR and SS acknowledge the support from the National Science Foundation-Binational Science Foundation (NSF-BSF, NSF no. MCB-2006154, BSF no. 2019723).

Conflict of Interests

The authors declare no conflict of interest.

Data Availability Statement

The data that support the findings of this study are available from the corresponding author upon reasonable request.

Keywords: CueR · EPR · CW-EPR · SDSL · Copper homeostasis

[1] a) R. A. Bonomo, D. Szabo, *Clin. Infect. Dis.* **2006**, *43 Suppl 2*, S49–56; b) J. Botelho, F. Grosso, L. Peixe, *Drug Resist. Updates* **2019**, *44*, 100640; c) W. Hwang, S. S. Yoon, *Sci. Rep.* **2019**, *9*, 487.
[2] a) G. M. Teitzel, M. R. Parsek, *Appl. Environ. Microbiol.* **2003**, *69*, 2313–2320; b) A. Pitondo-Silva, G. B. Goncalves, E. G. Stehling, *APMIS* **2016**, *124*, 681–688.
[3] a) G. Borkow, J. Gabbay, *Curr. Chem. Biol.* **2009**, *3*, 272–278; b) L. Hofmann, M. Hirsch, S. Ruthstein, *Int. J. Mol. Sci.* **2021**, *22*.
[4] a) J. M. Arguello, D. Raimunda, T. Padilla-Benavides, *Front. Cell. Infect. Microbiol.* **2013**, *3*, 73; b) D. Osman, J. S. Cavet, *Adv. Appl. Microbiol.* **2008**, *65*, 217–247.
[5] a) F. W. Outten, C. E. Outten, J. Hale, T. V. O'Halloran, *J. Biol. Chem.* **2000**, *275*, 31024–31029; b) L. Novoa-Aponte, D. Ramirez, J. M. Arguello, *J. Biol. Chem.* **2019**, *294*, 4934–4945.
[6] A. Changela, K. Chen, Y. Xue, J. Holschen, C. E. Outten, T. V. O'Halloran, A. Mondragon, *Science* **2003**, *301*, 1383–1387.
[7] D. Osman, C. Piergentili, J. Chen, B. Chakrabarti, A. W. Foster, E. Lurie-Luke, T. G. Huggins, N. J. Robinson, *J. Biol. Chem.* **2015**, *290*, 19806–19822.
[8] a) G. M. Teitzel, A. Geddie, S. K. De Long, M. J. Kirisits, M. Whiteley, M. R. Parsek, *J. Bacteriol.* **2006**, *188*, 7242–7256; b) J. Quintana, L. Novoa-Aponte, J. M. Arguello, *J. Biol. Chem.* **2017**, *292*, 15691–15704; c) J. T. Thaden, S. Lory, T. S. Gardner, *J. Bacteriol.* **2010**, *192*, 2557–2568.
[9] M. R. Wilkins, E. Gasteiger, A. Bairoch, J. C. Sanchez, K. L. Williams, R. D. Appel, D. F. Hochstrasser, *Methods Mol. Biol.* **1999**, *112*, 531–552.
[10] R. Schwartz, S. Ruthstein, D. T. Major, *J. Phys. Chem. B* **2021**, *125*, 9417–9425.
[11] a) J. V. Stoyanov, J. L. Hobman, N. L. Brown, *Mol. Microbiol.* **2001**, *39*, 502–511; b) J. Casto, A. Mandato, L. Hofmann, I. Yakobov, S. Ghosh, S. Ruthstein, S. K. Saxena, *Chem. Sci.* **2021**, *13*, 1693–1697.
[12] S. J. Philips, M. Canalizo-Hernandez, I. Yildirim, G. C. Schatz, A. Mondragon, T. V. O'Halloran, *Science* **2015**, *349*, 877–881.
[13] a) I. Yakobov, A. Mandato, L. Hofmann, K. Singewald, Y. Shenberger, L. Gevorkyan-Airapetov, S. Saxena, S. Ruthstein, *Protein Sci.* **2022**, *31*, e4309; b) H. Sameach, A. Narunsky, S. Azoulay-Ginsburg, L. Gevorkyan-Aiapetov, Y. Zehavi, Y. Moskovitz, T. Juven-Gershon, N. Ben-Tal, S. Ruthstein, *Structure* **2017**, *25*, 988–996 e983; c) H. Sameach, S. Ghosh, L. Gevorkyan-Airapetov, S. Saxena, S. Ruthstein, *Angew. Chem. Int. Ed. Engl.* **2019**, *58*, 3053–3056; d) L. Hofmann, A. Mandato, S. Saxena, S. Ruthstein, *Biophys Rev* **2022**, *14*, 1141–1159; e) Y. Igbaria-Jaber, L. Hofmann, L. Gevorkyan-Airapetov, Y. Shenberger, S. Ruthstein, *ACS Omega* **2023**, *8*, 39886–39895; f) M. Hirsch, L. Hofmann, Y. Shenberger, L. Gevorkyan-Airapetov, S. Ruthstein, *Biochemistry* **2023**, *62*, 797–807; g) L. Hofmann, S. Ruthstein, *J. Phys. Chem. B* **2022**, *126*, 7486–7494.
[14] T. Mima, H. Sekiya, T. Mizushima, T. Kuroda, T. Tsuchiya, *Microbiol. Immunol.* **2005**, *49*, 999–1002.
[15] Y. Choi, J. Koh, S. S. Cha, J. H. Roe, *Nucleic Acids Res.* **2024**, *52*, 4185–4197.
[16] D. J. Martell, C. P. Joshi, A. Gaballa, A. G. Santiago, T. Y. Chen, W. Jung, J. D. Helmann, P. Chen, *Proc. Natl. Acad. Sci. USA* **2015**, *112*, 13467–13472.
[17] a) H. M. McConnell, *In Foundations of Modern EPR*, World Scientific, **1998**; b) P. Z. Qin, K. Hideg, J. Feigon, W. L. Hubbell, *Biochemistry* **2003**, *42*, 6772–6783; c) W. L. Hubbell, H. S. McHaourab, C. Altenbach, M. A. Lietzow, *Structure* **1996**, *4*, 779–783; d) D. E. Budil, S. Lee, S. Saxena, J. H. Freed, *J. Magn. Reson. Ser. A* **1996**, *120*, 155–189.
[18] J. H. Freed, *In spin labeling (theory and applications)*, Academic press, New York, **1976**.
[19] a) L. Columbus, W. L. Hubbell, *Trends Biochem. Sci.* **2002**, *27*, 288–295; b) V. W. Cornish, D. R. Benson, C. A. Altenbach, K. Hideg, W. L. Hubbell, P. G. Schultz, *Proc. Nat. Acad. Sci.* **1994**, *91*, 2910–2914.
[20] S. Stoll, A. Schweiger, *J. Magn. Reson.* **2006**, *178*, 42–55.
[21] F. Torricella, A. Pierro, E. Mileo, V. Belle, A. Bonucci, *Biochim. Biophys. Acta Proteins Proteomics* **2021**, *1869*, 140653.
[22] R. K. Balogh, B. Gyurcsik, E. Hunyadi-Gulyas, J. Schell, P. W. Thulstrup, L. Hemmingsen, A. Jancso, *Chemistry* **2019**, *25*, 15030–15035.
[23] S. Crone, M. Vives-Florez, L. Kvich, A. M. Saunders, M. Malone, M. H. Nicolaisen, E. Martinez-Garcia, C. Rojas-Acosta, M. Catalina Gomez-Puerto, H. Calum, M. Whiteley, R. Kolter, T. Bjarnsholt, *APMIS* **2020**, *128*, 220–231.
[24] a) A. Waterhouse, M. Bertoni, S. Bienert, G. Studer, G. Tauriello, R. Gumienny, F. T. Heer, T. A. P. de Beer, C. Rempfer, L. Bordoli, R. Lepore, T. Schwede, *Nucleic Acids Res.* **2018**, *46*, W296–W303; b) S. Bienert, A. Waterhouse, T. A. de Beer, G. Tauriello, G. Studer, L. Bordoli, T. Schwede, *Nucleic Acids Res.* **2017**, *45*, D313–D319; c) N. Guex, M. C. Peitsch, T. Schwede, *Electrophoresis* **2009**, *30 Suppl 1*, S162–173; d) G. Studer, G. Tauriello, S. Bienert, M. Biasini, N. Johner, T. Schwede, *PLoS Comput. Biol.* **2021**, *17*, e1008667.

Manuscript received: March 26, 2024
Revised manuscript received: May 17, 2024
Accepted manuscript online: May 22, 2024
Version of record online: July 5, 2024